

ECE 445

SENIOR DESIGN LABORATORY

DESIGN DOCUMENT

Design Document

Wireless Fast Charging Autonomous Car

Team # 18

ZIYUE GUO (ziyueg3)
ZONGYANG ZHU (zz85)
YIZHI LI (yizhili2)
YIQUAN JIN (yiquanj2)

TA: YU DOU

March 27, 2024

Contents

1	Introduction	1
1.1	Problem	1
1.2	Solution	1
1.3	Visual Aid	2
1.4	External Systems	2
1.5	High-level Requirements List	2
2	Design	3
2.1	Diagram	3
2.1.1	Block Diagram	3
2.1.2	Physical Diagram	3
2.2	Subsystem Requirements and Verifications	5
2.2.1	Wireless Charging Subsystem	5
2.2.2	Drive Subsystem	8
2.2.3	Sensor Subsystem	9
2.2.4	Chassis Subsystem	10
2.2.5	Processor Subsystem	12
2.3	Subsystem Requirements	15
2.3.1	Wireless Charging Subsystem	15
2.3.2	Drive Subsystem	15
2.3.3	Sensor Subsystem	16
2.3.4	Chassis Subsystem	16
2.3.5	Processor Subsystem	16
2.4	Tolerance Analysis	16
2.4.1	Electrical Analysis	16
2.4.2	Mechanical Analysis	18
3	Cost and Schedule	21
3.1	Cost	21
3.1.1	Labor	21
3.1.2	Parts	21
3.1.3	Grand Total	22
3.2	Schedule	23
4	Ethics & Safety	25
4.1	Ethics Issues	25
4.2	Safety Issues	25
	References	27
A	Appendix A: Points Summary	28

1 Introduction

1.1 Problem

Current automobile vehicle is not completely auto since it can not go charging automatically when uses up electricity. Another problem is the current charger would occupy location so it may cause the waste of space. Our objective is to develop a vehicle that seamlessly integrates automatic wireless charging, autonomous navigation, and obstacle avoidance functionalities, enabling it to navigate its environment effortlessly while ensuring efficient energy replenishment.

Wireless charging cars may face several challenges. Efficiency loss due to electromagnetic interference and distance between coils is common, leading to slower charging and energy wastage. Precise alignment of charging coils is crucial, as misalignment affects charging efficiency. Interference from electronic devices and obstacles can disrupt charging. Heat generation during charging sessions poses risks to battery health. Compatibility issues between different charging standards hinder widespread adoption. Balancing range, efficiency, and battery size is crucial for optimizing wireless charging in electric vehicles.

1.2 Solution

A proposal is put forth for the development of an autonomous vehicle equipped with wireless fast charging capability ($P_{in} \geq 100W$). This vehicle is designed to autonomously detect the location of wireless charging stations and navigate to them swiftly and efficiently. In addition, the proposed autonomous vehicle will incorporate computer vision technology to enable obstacle avoidance, further enhancing its navigational capabilities. To save the space, the charging system is set at the ground of the vehicle instead of standing at the side of the vehicle.

Using supercapacitors instead of lithium-ion batteries at the receiver end of wireless charging coils offers several advantages. Supercapacitors provide rapid charging and discharging capabilities, with precise control over the magnitude of current flow. This allows for quick energy storage and release during short charging sessions while ensuring efficient energy management. Additionally, supercapacitors offer enhanced safety, and durability compared to lithium-ion batteries. Overall, integrating supercapacitors into wireless charging systems improves reliability, safety, and sustainability while enabling precise control over current flow for optimized energy storage.

1.3 Visual Aid

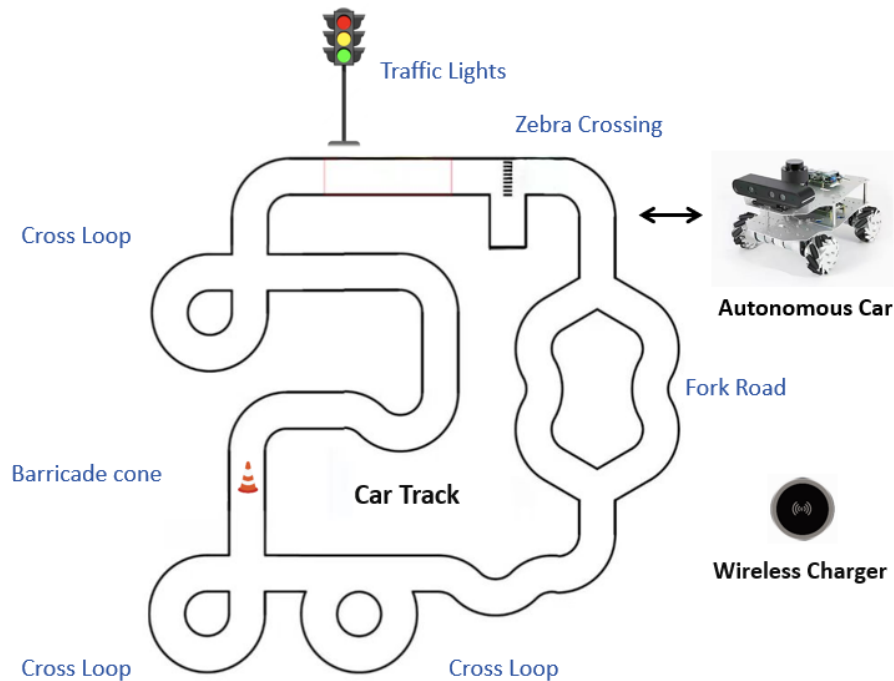


Figure 1: **Visual Aid.** This diagram combines our visual aids, including a driving map, a wireless charger on the ground, and the vehicle.

1.4 External Systems

We require both a ground-based charging station and a detailed map for the vehicle's navigation purposes.

The requirements of the driving map will be stated below. The car should be stopped when recognizing the traffic lights. When recognizing the zebra crossing, it should be slowed down. When passing through the curve or cross loop, you should not touch the wall. Finally, when you recognize the barricade zone, it is determined to reach the target, and automatically go to the charging point for wireless charging.

1.5 High-level Requirements List

- The wireless charging power $P_{in} \geq 100W$.
- Car can automatically align to the charging coils.
- Car can detect the place of wireless charging station.
- The overall size of the car is around 266mm×230mm×202mm.

2 Design

2.1 Diagram

2.1.1 Block Diagram

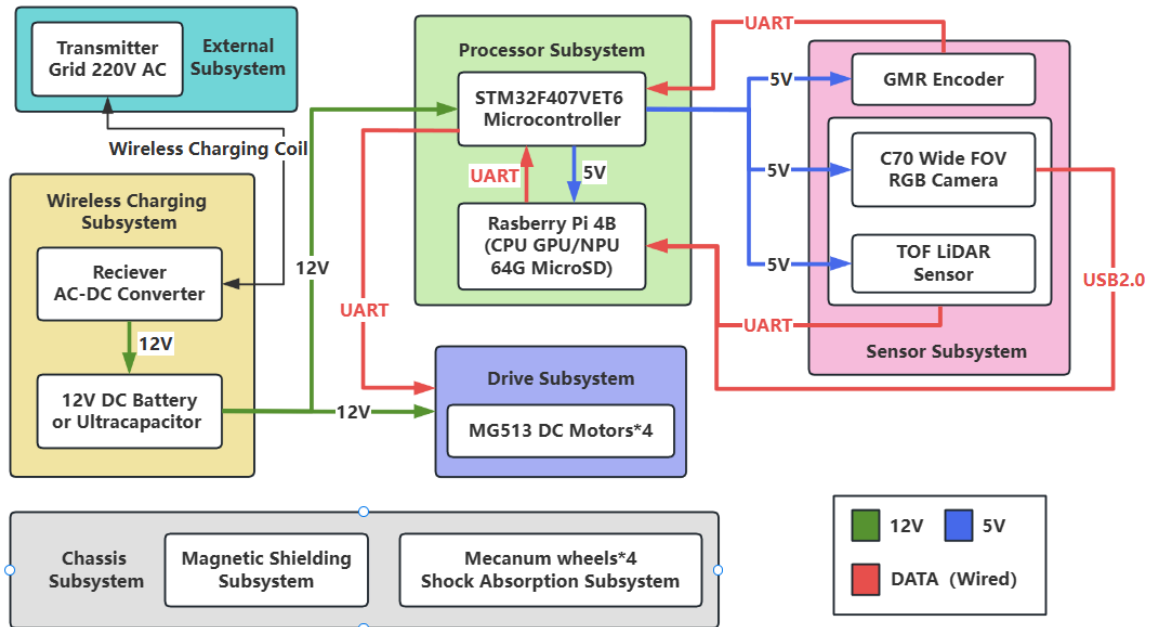


Figure 2: Block Diagram

2.1.2 Physical Diagram

Figure 3 below is the initial CAD model of the cart. The main body of the cart consists of a two-tier carbon steel platform and four McNamee wheels. The McNamee wheels and battery pack are mounted on the carbon steel chassis below. The depth camera and radar are mounted on the carbon steel platform above.

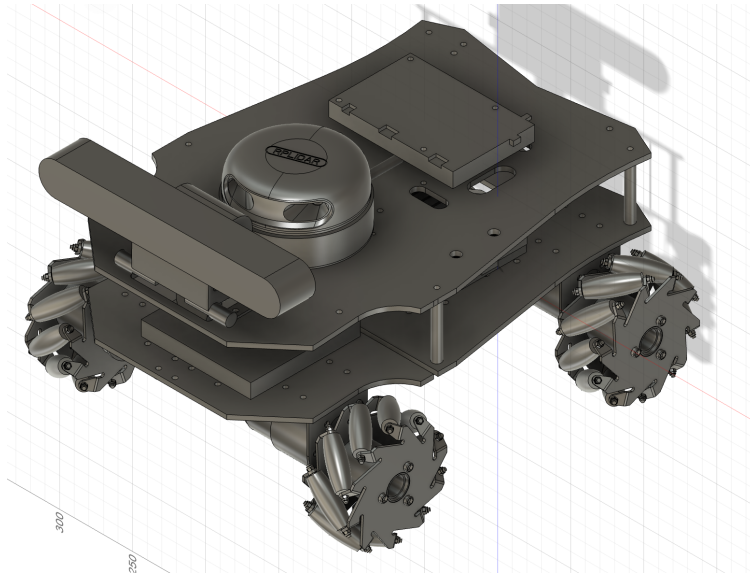


Figure 3: Physical Diagram

Our goal is to build a compact model of a cart that can be made capable of automatic sign recognition, automatic trajectory and high power wireless charging. Figure 4 below is a three view of the initial cart model. In order to reduce the size of the cart on the basis of ensuring the reasonable installation of the cart components, the area of our carbon steel platform is 372.46 cm^2 . The platform can accommodate four McNamee wheels and their mounting components, as well as the depth camera, radar and main control board at the same time.

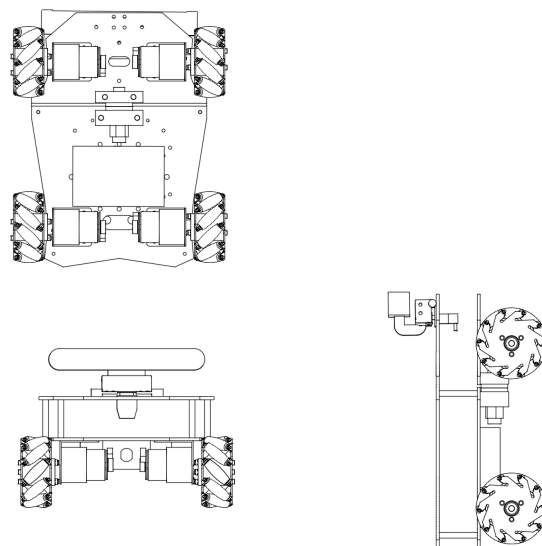


Figure 4: Three Views of Model

2.2 Subsystem Requirements and Verifications

2.2.1 Wireless Charging Subsystem

The wireless charging subsystem mainly consists of two parts: the transmitter and the receiver. At the transmitter end, it first connects to the grid, and after passing through a rectifier, converts AC electricity into DC. Next, the DC power is converted back to AC through an inverter, ensuring that the frequency of the AC power meets the requirements for wireless charging. When power is supplied, an alternating electromagnetic field is generated near the primary coil at the transmitter end. Equipped on the electric vehicle, the receiver includes a secondary coil to capture the energy from the oscillating magnetic field. The receiver mainly consists of a rectifier, with its output connected to the vehicle's DC battery. Once the vehicle is parked over the base station, it receives the oscillating magnetic field. The changing magnetic field induces a current in the vehicle's secondary coil.

Furthermore, to maximize charging power, the vehicle first utilizes the Maximum Power Point Tracking (MPPT) algorithm to locate the optimal charging position. The implementation of the MPPT algorithm is based on Raspberry Pi. Once the vehicle moves to the expected position, charging begins.

It is worth noting that we must ensure the safety of the charging process to prevent dangers such as overcharging of the battery or circuit short circuits. Therefore, we will incorporate current and voltage samplers as well as a relay into the receiver circuit, which can detect circuit data in real-time and disconnect the circuit promptly in the event of an emergency. We have completed the design of a portion of the PCB circuit, and its schematic and layout are shown below. (Fig. 5 6)

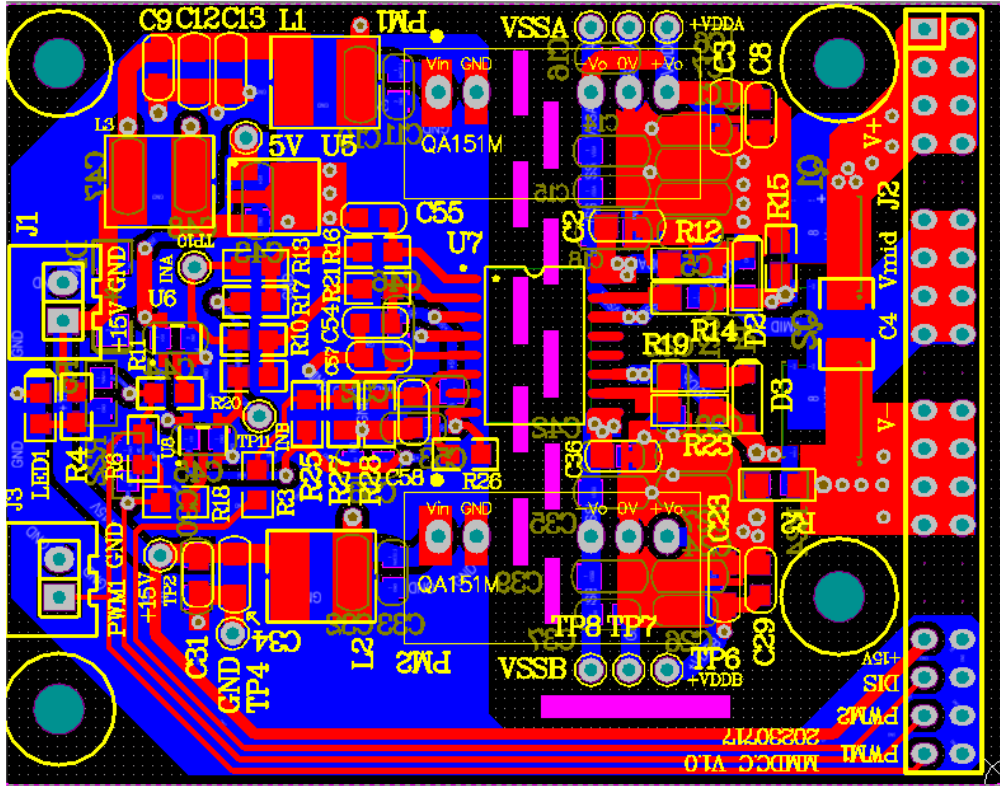
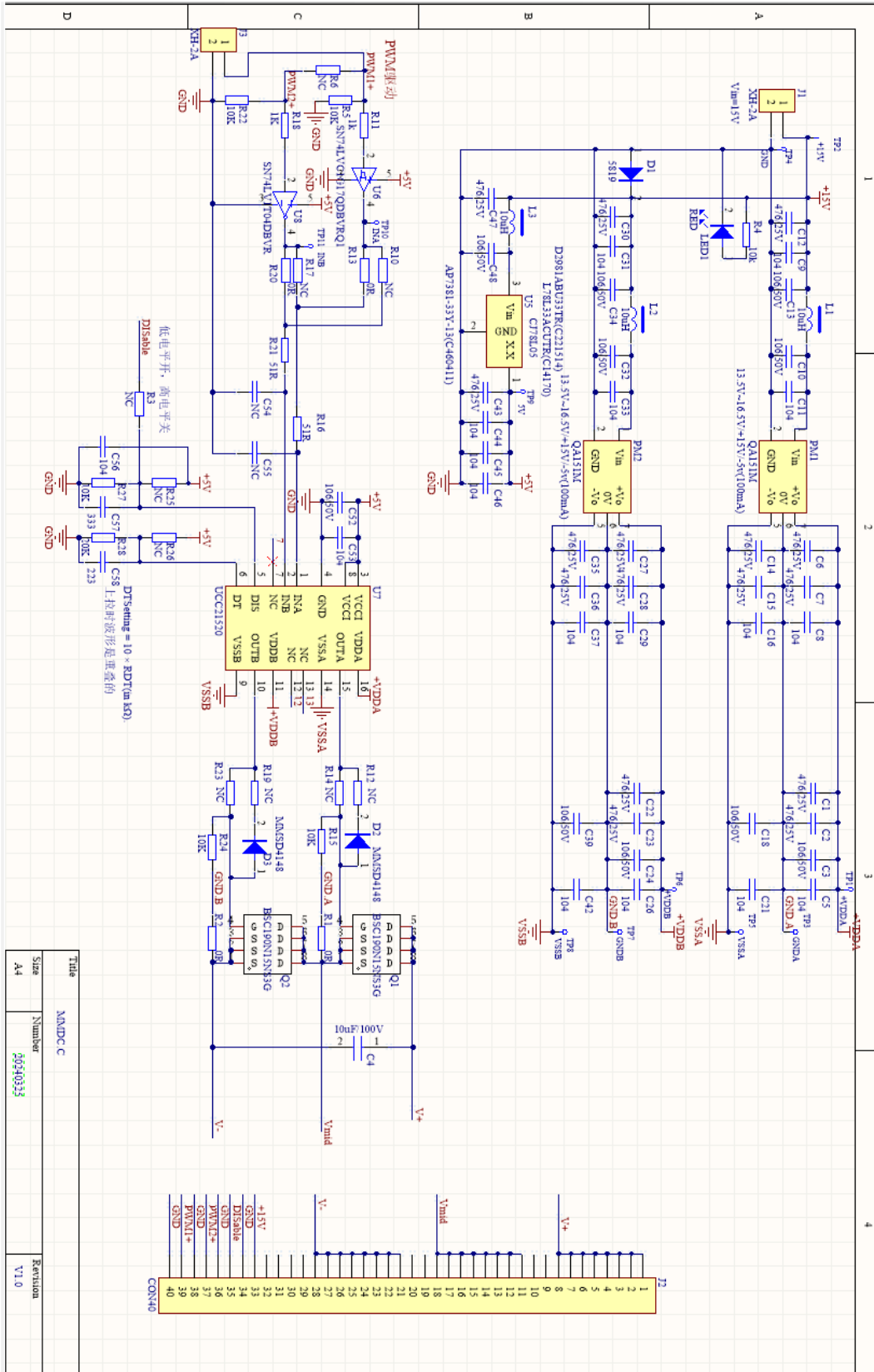


Figure 5: Layout PCB Design (Partial)



Title	MANDC C	Revision
Size	Number	
A4	20240323	V1.0

Figure 6: Schematic PCB Design (Partial)

Requirements	Verification
1) Implement fast wireless charging with 100W power.	1) Measure the voltage and current of the primary and secondary coils and measure the transmission efficiency. Measure the time it takes for the current to stabilize to determine the charging time.
2) Ensure the safety of the charging process to prevent dangers such as overcharging of the battery or circuit short circuits.	2) Use a multimeter and an oscilloscope to test whether the relay protection function is working properly.
3) The MPPT algorithm is used to find the position with the maximum charging power to maximize the efficiency of wireless charging.	3) Find the maximum accepted power and compare it with simulink simulation theory value.

2.2.2 Drive Subsystem

The drive subsystem of the intelligent car responds rapidly to instructions provided by the processor system and ensures smooth and accurate control over the car's movement in various directions, including forward, backward, left, right, and even turning in place. The drive subsystem primarily consists of the MG513 metal gear reduction motor, clamping type couplers, motor brackets, and other components. The four motors are mechanically connected to the four Mecanum wheels and mounted on the chassis subsystem, powered by the power subsystem, and controlled by the processor subsystem. Specifically, the car requires four DC reduction motors (Fig. 7), consisting of full-metal gear reduction boxes and GMR encoders from the sensor subsystem. The selected motors have a rated voltage of 12V, a rated current of 0.36A, a reduction ratio of 30, and a power of approximately 4W. The rated torque of the motors is 1kg.cm, and the unloaded speed after reduction is 366 ± 26 rpm. We estimate that the motors can drive the car at a maximum speed of approximately 1.2m/s and can carry a maximum weight of 3-4kg, which fully meets our requirements.

The critical code for the drive motor is below:

```
void Drive_Motor (float wx, float vy, float vz)
{
    MotorTarget.A = (vx+vy-vz*(Wheel_spacing+Wheel_axlespacing));
    MotorTarget.B = (vx-vy-vz*(Wheel_spacing+Wheel_axlespacing));
    MotorTarget.C = (vx+vy+vz*(Wheel_spacing+Wheel_axlespacing));
    MotorTarget.D = (vx-vy+vz*(Wheel_spacing+Wheel_axlespacing));
}
```

}



Figure 7: MG513P30_12V DC motor

Requirements	Verification
1) Use four PWM drives to independently adjust the speed and direction of the four motors.	1) Use oscilloscope to check the current passing the motor. When the current is positive, the motor rotates clockwise.
2) The rated power of the designed motor is 4.32W and the rated torque is 1kg*cm	2) Test the speed and kinetic energy of the car to calculate the actual power.

2.2.3 Sensor Subsystem

ASTRA S RGBD depth camera The ASTRA S RGBD camera is a type of camera used to capture RGB (color) and depth information simultaneously. This camera can capture both color images and depth information for each pixel, typically achieved using infrared or other depth sensing technology. By combining RGB and depth information, it enables more accurate object detection, tracking, pose estimation, and other tasks, while also aiding in the creation of more realistic virtual environments or augmented reality applications.

The ASTRA S RGBD camera features a depth range of 0.4 to 2.0 meters, with a power consumption of less than 2W and a peak current of under 500mA. Its depth field of view spans horizontally at 58.4 degrees and vertically at 45.5 degrees, while the color field of view extends horizontally at 63.1 degrees and vertically at 49.4 degrees. Data transmission is facilitated via USB 2.0 connectivity.

Leishen N10P radar We will employ the Leishen N10P radar sensor to facilitate obstacle avoidance functionality, which is a commercial-grade Time-of-Flight (TOF) LiDAR sensor, with a measurement range of 25 meters, a sampling frequency of 5400Hz, and a serial interface for communication. This radar will be employed to detect obstacles on both

sides and in front of the vehicle, including roadblocks and walls, allowing for timely adjustments to the vehicle’s trajectory as necessary.

Giant Magnetoresistive encoder For obstacle avoidance function, the GMR (Giant Magnetoresistive) encoder can help the intelligent car accurately identify obstacles and perform obstacle avoidance operations, thereby ensuring safe driving. And it can also help intelligent vehicles achieve path planning and autonomous navigation, enabling them to autonomously travel and complete tasks in complex environments. The rated voltage is about 5V.

Requirements	Verification
1) Ensure that the power supply interface is correct and the current is safe and stable.	1) Data transmission is facilitated via USB 2.0 connectivity. Other parameters also need to be matched with each sensor.
2) Ensure that the camera can identify surrounding environments in real-time, discerning patterns such as zebra crossings and traffic lights.	2) We will initially conduct photo tests using the camera to evaluate whether its resolution, field of view (FOV), and other parameters meet requirements. The captured images will then be uploaded to an image recognition algorithm to assess its accuracy in detection.
3) Ensure the radar can detect surrounding obstacles and transmit signals to the processor	3) Use an oscilloscope to test whether the radar output signal is normal.

2.2.4 Chassis Subsystem

Shock Absorption Subsystem The design of this shock structure (Fig. 8) takes its cues from the McPherson suspension, which is a combination of a wishbone and a candle suspension. In this structure, the main support structure in the center assumes the role of connecting the four cross arms to the base of the trolley. The four cross-arms are divided into two groups that extend from each side of the center support. The cross arm located below is connected to the center stand by means of an oil-hydraulic shock absorber TRX4 SCX10 90046, thus enabling the four Mecanum wheels to independently realize the shock absorption function in complex terrains.

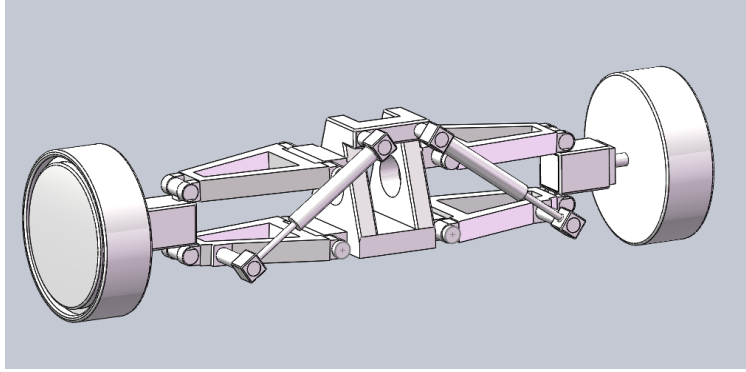


Figure 8: Shock Absorption Structure

Requirements	Verification
<p>1) Maintaining the relative level of the cart chassis on uneven ground improves wireless charging efficiency.</p>	<p>1) A: The cart-mounted shock absorbing structure was placed on a test surface with level ground on the left and a ten-degree slope on the right. B: Calculate the wireless charging efficiency, which is above eighty-five percent.</p>
<p>2) Maintaining the stability of the overall attitude of the cart ensures the efficiency and accuracy of the depth camera recognition.</p>	<p>2) A: The cart-mounted shock absorbing structure was placed on a test surface with level ground on the left and a ten-degree slope on the right. B: Observe the camera recognition, the camera recognizes the roadway and signs ahead normally.</p>

Magnetic Shielding Subsystem The material to isolate the magnetic field will be placed above the wireless charging structure in the chassis of the cart to protect the control system components of the main body of the cart, preventing the magnetic field during high power wireless charging from having an effect on the circuitry components, which can affect the control of the cart.

Requirements	Verification
1) Isolates electromagnetic waves during wireless charging to protect circuit components and ensure normal circuit operation.	1) A: Install magnetically shielded components and place the cart as a whole in a 100W electromagnetic wave environment. B: Observe the operation of the circuit and controller to ensure that the circuit operates normally.

2.2.5 Processor Subsystem

Raspberry Pi 4B Our ROS (Robot Operating System) controller is based on the Raspberry Pi 4B, featuring a quad-core ARM Cortex-A72 processor clocked at 1.5GHz, 4GB of RAM, with a computational power of 0.2 TOPS. It operates on a 5V power supply. (Fig. 9)

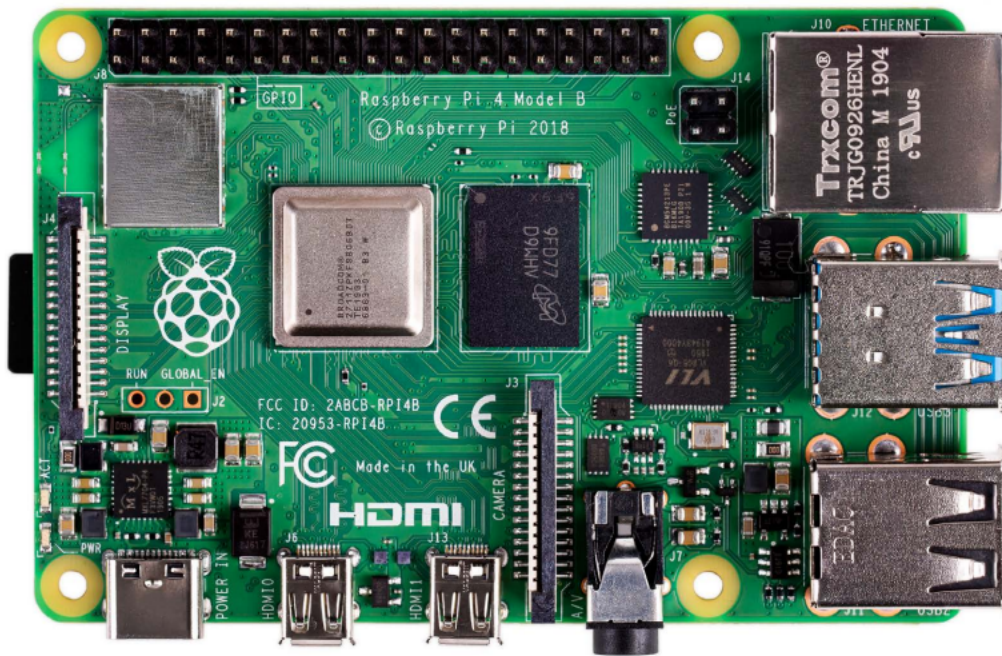


Figure 9: Raspberry Pi 4B

The ROS controller, running on the Raspberry Pi 4B, establishes connections and controls the camera and LiDAR sensor via their respective interfaces. The camera, operating through a USB 2.0 connection and supporting the UVC standard, streams RGB images

to the Raspberry Pi. These images are processed using ROS-compliant computer vision algorithms.

STM32 microcontroller Furthermore, we use the STM32 microcontroller to provide supply voltage to the Raspberry Pi 4B and the sensor subsystem and receive data from them. The STM32 microcontroller can also provide control signal to the drive subsystem. (Fig. 10)

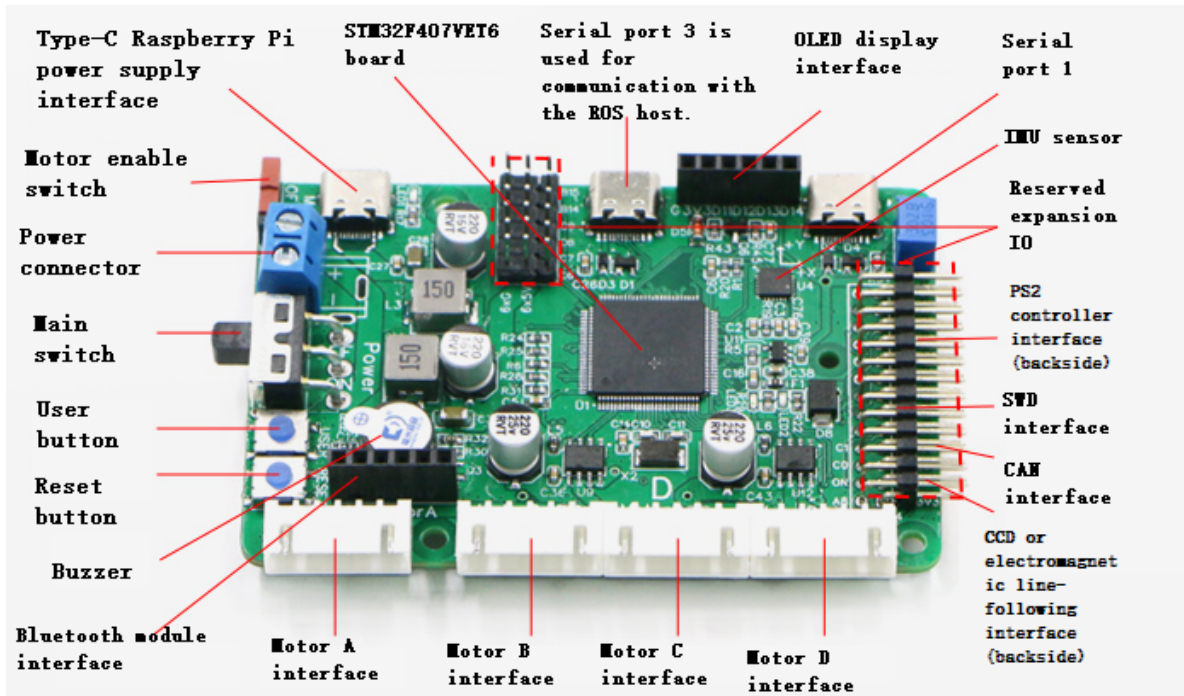


Figure 10: STM32 microcontroller

Leishen N10P LiDAR sensor On the other hand, the LiDAR sensor, the Leishen N10P, communicates with the Raspberry Pi via a serial interface. The ROS controller sends commands to the LiDAR sensor to initiate measurements and receives distance data back from the sensor. This data is then processed to detect obstacles and adjust the vehicle’s navigation path as required.

In summary, the ROS controller orchestrates the interaction between the Raspberry Pi and the camera/LiDAR sensor, receiving data from these sensors, processing it, and making control decisions for the autonomous vehicle’s navigation and charging operations.

Component Wiring STM32 Controller Integrated Dual 5V Power Supplies: The STM32 controller is equipped with two 5V power outputs. One 5V power supply powers the STM32 controller and peripherals (such as encoders, Bluetooth, gamepads, etc.), while the other 5V power supply is used to power the Raspberry Pi.

- Raspberry Pi Power Supply (Fig. 11): The 5V power circuit of the Raspberry Pi is integrated into the STM32 controller's adapter board, utilizing a Type-C to Type-C cable capable of delivering over 3A of current.



Figure 11: **Raspberry Pi Power Supply Wiring**

- Communication between Raspberry Pi and STM32 Controller (Fig. 12): As the Raspberry Pi acts as the host machine communicating with the STM32 controller, the default choice is the integrated UART 3, which features the CP2102 level conversion chip.

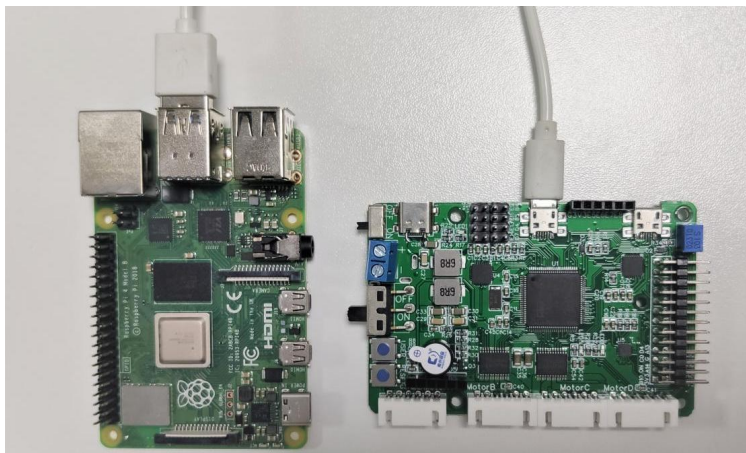


Figure 12: **Communication Between Raspberry Pi and STM32**

- Raspberry Pi Connection to Navigation Radar (Fig. 13): A standard Micro-USB cable is used for the connection between the Raspberry Pi and the LiDAR sensor. While providing power to the LiDAR sensor, the Raspberry Pi also communicates with it.

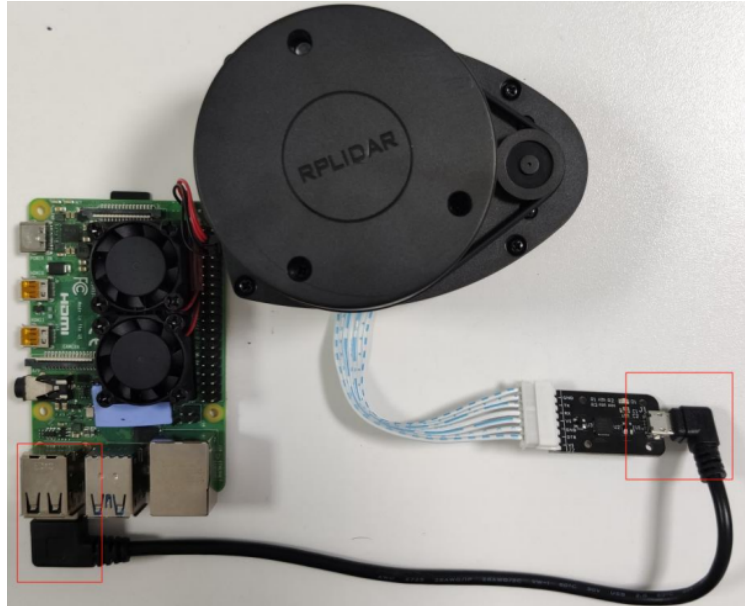


Figure 13: Raspberry Pi Connection to Navigation Radar

Requirements	Verification
1) The components need to be connected to the power supply normally and ensure communication with each other	1) The STM32 controller is equipped with two 5V power outputs. One powers the STM32 controller and peripherals, while the other is used to power the Raspberry Pi.
2) Ensure that the power supply interface is correct and the current is safe and stable	2) For Raspberry Pi, utilize a Type-C to Type-C cable capable of delivering over 3A of current.

2.3 Subsystem Requirements

2.3.1 Wireless Charging Subsystem

- 12V 5000mAh Lithium Battery
- 220V/20V Rectifier
- 20V/12V Converter
- 100W Wireless Charging Coil Transmitter

2.3.2 Drive Subsystem

- MG513P30_12V DC Metal Gear Reduction Motor

2.3.3 Sensor Subsystem

- ASTRA S RGBD camera
- Leishen N10P Time-of-Flight (TOF) LiDAR sensor
- GMR Encoder

2.3.4 Chassis Subsystem

- All-metal dual-stage spring-loaded hydraulic shock absorbers.
- Ferrite material: Ferrite is a ceramic material with spin magnetic moment, which has high magnetic field permeability, high magnetic permeability, and high magnetic saturation strength, and can effectively isolate high frequency electromagnetic waves and magnetic fields.

2.3.5 Processor Subsystem

- STM32F407VET6 Microcontroller
- Raspberry Pi 4B(CPU GPU/NPU 64G MicroSD)

2.4 Tolerance Analysis

2.4.1 Electrical Analysis

Considering the wireless charging requirements in our project, we identify the wireless charging subsystem as the area most susceptible to risks. We are concerned that the current-voltage ripple in the charging circuit may affect the normal operation of other subsystems, posing a significant demand for debugging the inductor and capacitor in the circuit. Below is the schematic simulation of the wireless charging section conducted in MATLAB Simulink. We have omitted the circuit for rectifying 220V AC into DC. Our simulated circuit includes a high-frequency inverter and a rectifier (Fig. 14).

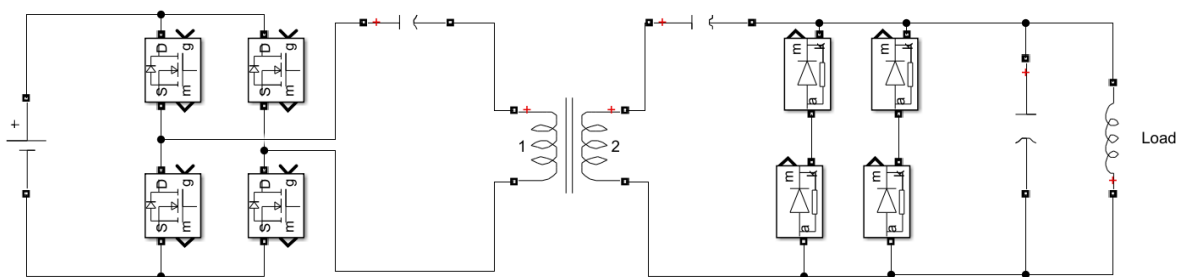


Figure 14: Schematic simulation circuit of part of the wireless charging subsystem

For the left-side inverter circuit:

$$V_{out} = \frac{4V_{in}}{\pi} \cos \frac{\delta}{2} \cos(\omega_{out}t - \frac{\delta}{2})$$

where V_{in} is the DC input voltage, V_{out} is the output voltage, ω_{out} is the angular frequency of the high-frequency AC, and δ is the displacement angle.

For the right-side rectifier circuit:

$$\Delta V_{out} \leq \frac{V_O}{2fRC}$$

$$C \approx \frac{V_O}{2fR\Delta V_{out}}$$

where ΔV_{out} is the DC output ripple voltage, V_O is the peak voltage of the AC, f is the frequency of the AC, R and C are the resistor and capacitor on the output side of the circuit, respectively. We adjust the size of the capacitor to minimize the ripple voltage.

We conducted initial simulation (Fig. 15) and debugging of the output voltage at the receiver end using Simulink. The results are shown in the following figure. The output voltage is 12V, and the voltage ripple is within an acceptable range.

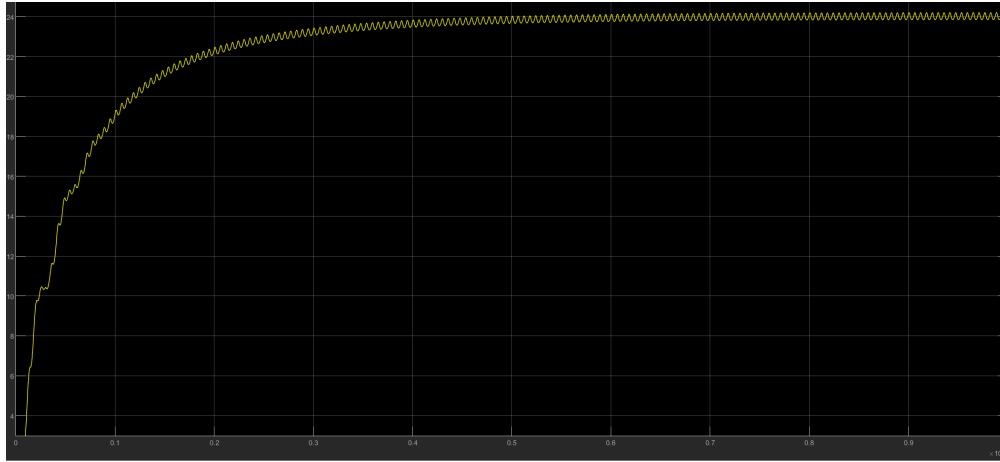


Figure 15: The simulation of the output voltage at the receiver end.

We have not provided specific values for the capacitance, resistance, and inductance in the circuit yet because the internal resistance and impedance of coils and other electronic components are unknown. This requires adjustment in our laboratory experiments. We are also concerned about the possibility of damaging the battery due to excessive peak voltage during wireless charging. It is important to emphasize the safety of the charging process to mitigate risks such as battery overcharging or circuit short circuits. Hence, we plan to integrate current and voltage sensors along with a relay into the receiver circuit. These components will monitor circuit conditions in real-time and swiftly disconnect the circuit in case of an emergency.

2.4.2 Mechanical Analysis

The Mecanum Wheel consists of a hub and many small rollers fixed around its periphery, typically at a 45° angle between the wheel axis and the roller axis. Each wheel has three degrees of freedom: rotation about the wheel axis, movement along the roller axis perpendicular to the ground, and rotation about the contact point between the wheel and the ground. According to mechanical principles, the number of input components should equal the degrees of freedom of the mechanism. Therefore, to achieve control of three degrees of freedom, there should be three independent inputs. Since each Mecanum wheel can be considered a driving element, to achieve control of three degrees of freedom in a plane, there should be at least three Mecanum wheels. In other words, theoretically, a mobile platform composed of three such wheels can achieve omnidirectional movement. However, in practical applications, Mecanum wheels are typically used in pairs: two left-handed and two right-handed wheels, totaling four. The left-handed and right-handed wheels are chirality symmetric, which increases the stability of the mechanism, facilitates control, and enhances the load capacity. According to the inverse kinematics formula of the robot, we can calculate the target speed of the wheel

$$V_X = \frac{V_A + V_B + V_C + V_D}{4}$$

$$V_Y = \frac{V_A - V_B + V_C - V_D}{4}$$

$$V_Z = \frac{-V_A - V_B + V_C + V_D}{4}$$

where V_X is forward and backward speed, V_Y is side to side speed, V_Z is speed of rotation on axis. V_A , V_B , V_C , and V_D are linear speed of the wheels.

Considering the weight of the trolley's carbon steel platform and individual components, we need to perform Finite Element Analysis of the right-angle connectors between the carbon steel chassis and the motor, as well as the flanged metal connectors between the motor drive shaft and the McNamee wheel.

Figure 16 shows the stress distribution of right angle connectors, Figure 17 shows the deformation displacement of right angle connectors, Figure 18 shows the stress distribution of flanged metal connectors, and Figure 19 shows the deformation displacement of flanged metal connectors. The materials of this connection are all carbon steel. Carbon steel is a metal material mainly composed of iron and carbon, carbon steel has high hardness and strength, excellent processing performance and has elasticity and not easy to break. Therefore, carbon steel is the ideal material to realize our design. From Figure 17 we can see that the maximum displacement of the right-angle connector under stress is 0.095mm, which meets the design requirements. From Figure 19, we can see that the maximum displacement of the flanged metal connection under stress is 3.967E-05mm, which also meets the design requirements.

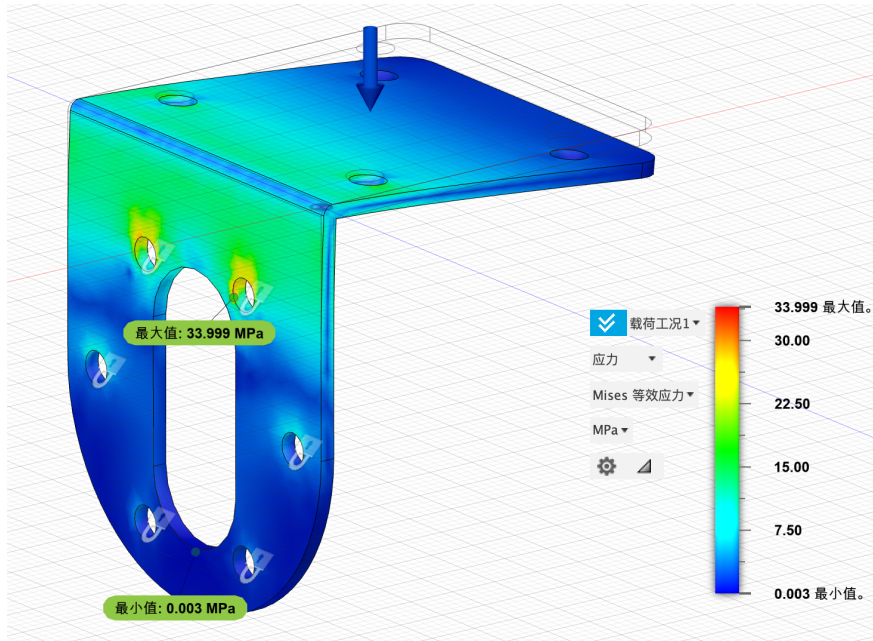


Figure 16: Right-Angle Connectors Stress

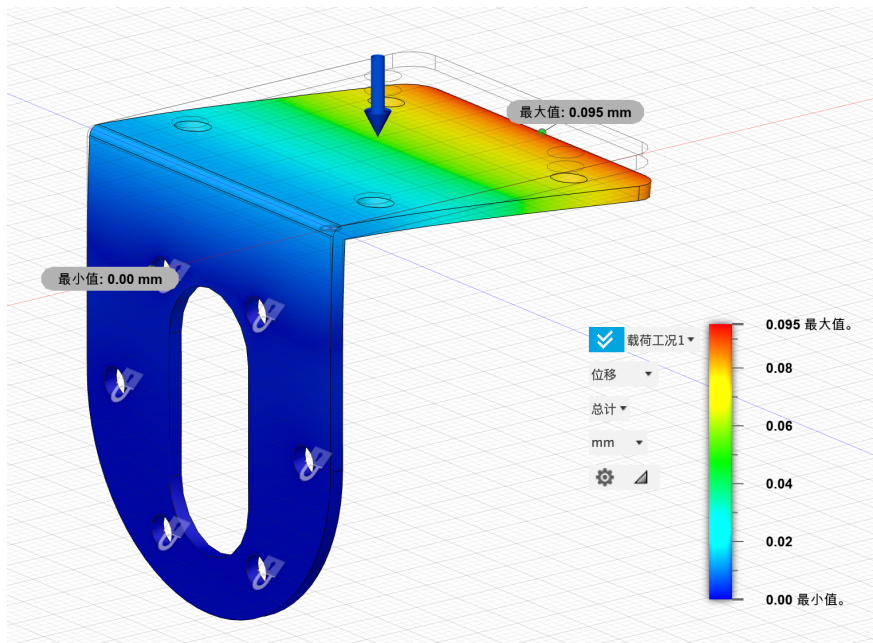


Figure 17: Right-Angle Connectors Displacement

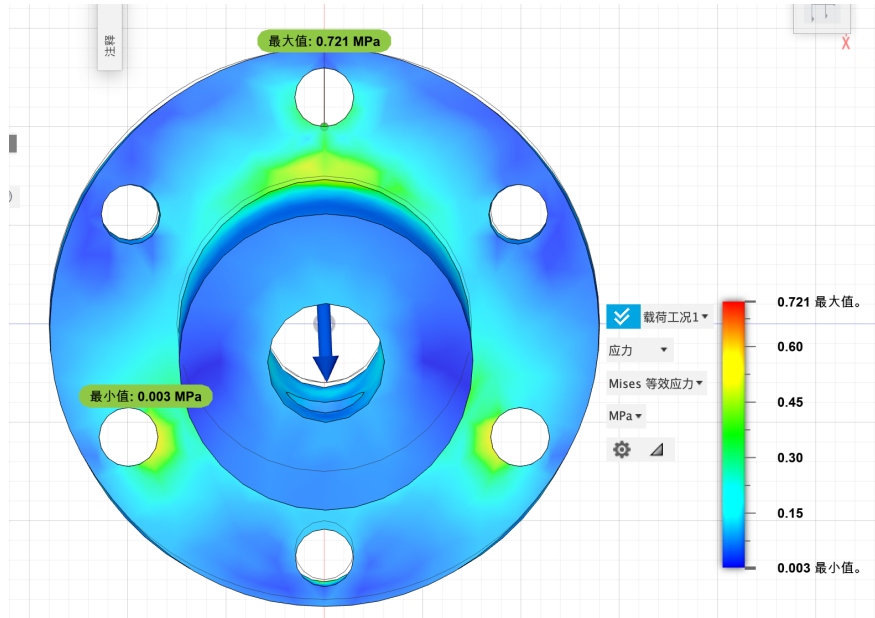


Figure 18: Flanged Metal Connectors Stress

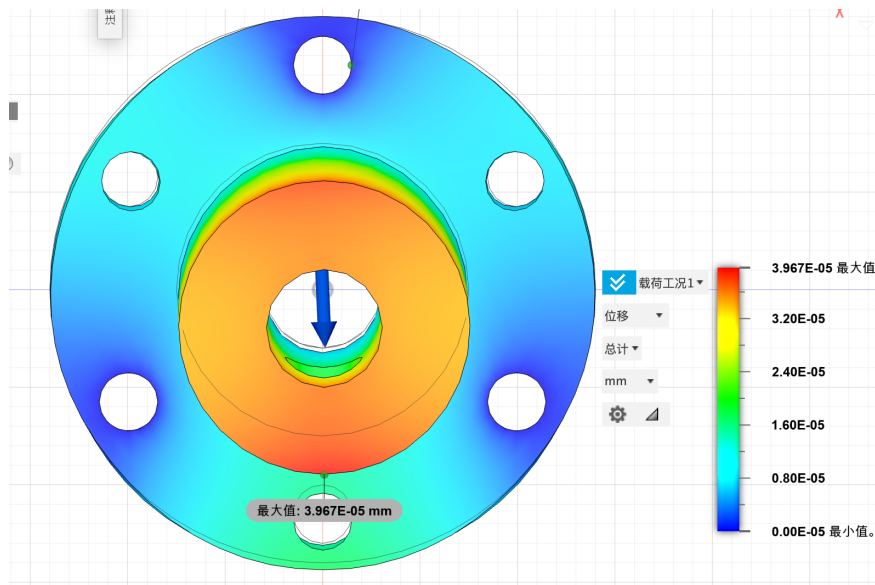


Figure 19: Flanged Metal Connectors Displacement

3 Cost and Schedule

3.1 Cost

3.1.1 Labor

The labor cost for our project is as follows (Tab. 3.1.1): We have selected the average salary of UIUC graduates as our hourly wage, which amounts to \$35 per hour. Subsequently, we estimate the total working hours required to complete the project based on our workload and course credits. Assuming a reasonable salary, the calculation is as follows: (\$35/hour) x 2.5 x hours to complete = TOTAL.

Member	\$/Hrs	Hrs/Week	Weeks	Multiplier	Total
ZIYUE GUO	35	20	14	2.5	\$24,500
ZONGYANG ZHU	35	20	14	2.5	\$24,500
YIZHI LI	35	20	14	2.5	\$24,500
YIQUAN JIN	35	20	14	2.5	\$24,500
TOTAL	140	20	14	2.5	\$98,000

Table 1: Labor Cost Analysis

3.1.2 Parts

The following (Tab. 3.1.2) is a table listing all hardware parts (description, manufacturer, part #, quantity, and cost). We estimate the hardware cost to be ¥ 3958, which is approximately \$548.

Name	Description	Manufacturer	Part #	Quantity	Cost	Total
Battery	12V 5000mAh DC Lithium Battery	WHEELTECH	E353S	1	¥ 119	¥ 119
Wireless Charging Coils	100W24V4A high-power and high-efficiency wireless charging Coils	WP	WP3640T WP2450R	1	¥ 120	¥ 120
Motor	12V DC Metal Gear Reduction Motor	WHEELTECH	MG513P30	4	¥ 79	¥ 316
Camera	ASTRA S RGBD Camera	ORBEC	ASTRA S RGBD	1	¥ 960	¥ 960
Radar Sensor	Time-of-Flight (TOF) LiDAR sensor	LEISHEN	N10P	1	¥ 479	¥ 479
Micro-controller STM32	C30D ROS Four Wheel Drive MCU	ST-Microelectronics	STM32-F407VET6	1	¥ 379	¥ 379
Raspberry Pi 4B	Raspberry Pi 4B (CPU GPU/NPU 64G MicroSD)	Raspberry Pi	Raspberry Pi 4B	1	¥ 778	¥ 778
Chassis	R3 Series Four-wheel Drive Chassis	WHELLTEC	R3S	1	¥ 759	¥ 759
Shock Absorber	Oil Pressure Shock Absorber 75mm	Riaario	AM-X12	2	¥ 24	¥ 48
Total						¥ 3958

Table 2: Hardware Cost Analysis

3.1.3 Grand Total

We add up all the costs mentioned above, and we get $\$98,000 + \$548 = \$98,548$.

3.2 Schedule

Week	Task	Responsibility
03/25/2024	Completion of research on lithium battery for charging.	ZIYUE GUO
	Simulate and test the wireless charging circuit.	ZONGYANG ZHU
	Research on CV recognition models for the equipped chip.	YIZHI LI
	Complete the improvement of the shock absorption system.	YIQUAN JIN
04/01/2024	Firstly utilize lithium batteries to complete the debugging of the control and operating systems.	ZIYUE GUO
	Build the corresponding PCB circuits for wireless charging and DC converter.	ZONGYANG ZHU
	Combine CV recognition models and radar to cope with the complex driving map.	YIZHI LI
	Complete the Chassis system.	YIQUAN JIN
04/08/2024	Finish the components and connection of PWM motor drive.	ZIYUE GUO
	Finish the calibration of coils for charging station and vehicle.	ZONGYANG ZHU
	Train the dataset of traffic and charging signs to improve the CV framework.	YIZHI LI
	Printing shock absorption system components and trying to assemble the shock absorption system using a 3D printer.	YIQUAN JIN
04/15/2024	Implement charging and controlling of the motor drive fluently.	ZIYUE GUO
	Build converter and rectifier to adjust the voltage for various parts.	ZONGYANG ZHU
	Implement the MPPT algorithm based on Raspberry Pi 4B.	YIZHI LI

	Purchase and cut the magnetoresistive material and mount the magnetoresistive structure to the chassis.	YIQUAN JIN
04/22/2024	Embed four motors in the car and connect to the STM32.	ZIYUE GUO
	Embed the wireless charging system into the vehicle.	ZONGYANG ZHU
	Optimize the programs of tracking and recognition to reduce the computing complexity.	YIZHI LI
	Improvement of the structure of the shock-absorbing system and assembly of a new shock-absorbing system.	YIQUAN JIN
04/29/2024	Fix bugs & Integration testing & Prepare Mock Demo.	ZIYUE GUO
	Fix bugs & Integration testing on the wireless charging subsystem.	ZONGYANG ZHU
	Fix bugs & Integration testing on the path-finding subsystem.	YIZHI LI
	Consolidate the shock-absorbing system into the vehicle	YIQUAN JIN
05/06/2024	Integrate the whole system and debug.	ZIYUE GUO
	Integrate the whole system and debug.	ZONGYANG ZHU
	Finish product tests and iterations.	YIZHI LI
	Finish product tests and iterations.	YIQUAN JIN
05/13/2024	Work on the final report and prepare for the demo.	ZIYUE GUO
	Work on the final report and prepare for the demo.	ZONGYANG ZHU
	Work on the final report and prepare for the demo.	YIZHI LI
	Work on the final report and prepare for the demo.	YIQUAN JIN

4 Ethics & Safety

4.1 Ethics Issues

Ethical Issues of High-Power Wireless Charging Autonomous Vehicles:

1. **Privacy Concerns:** The wireless charging system may require communication with the vehicle to better manage the charging process. This communication may involve information such as the vehicle's location and driving habits. Ensuring the privacy of this data, preventing misuse, and unauthorized access raises ethical considerations regarding user privacy [1]. We promise that our project will adopt security measures according to law so as to not invade user's privacy by following the ACM Code of Ethics, 1.6, "taking precautions to prevent re-identification of anonymized data or unauthorized data collection, ensuring the accuracy of data, understanding the provenance of the data, and protecting it from unauthorized access and accidental disclosure." [2]
2. **Social Equity:** The widespread adoption of high-power wireless charging technology may face issues of social equity. If the implementation of this technology is predominantly limited to specific regions or socioeconomic groups, it could exacerbate technological divides, leading to ethical concerns related to social fairness.
3. **Emergency Handling:** In emergency situations such as fires or accidents, the ethical responsibility for safely interrupting the charging process and ensuring the safety of the vehicle and the surrounding environment comes into play.

4.2 Safety Issues

Safety Issues of High-Power Wireless Charging Autonomous Vehicles:

1. **Electromagnetic Radiation:** High-power wireless charging systems may generate strong electromagnetic radiation, posing safety risks to individuals, animals, and other electronic devices. Ensuring that the system complies with relevant electromagnetic radiation safety standards is critical to reducing potential health risks.
2. **Charging Speed and Battery Life:** Pursuing excessively fast charging speeds may negatively impact battery life and performance. Safety-wise, it is necessary to balance charging speed and battery health to ensure the safe operation of the vehicle and preserve battery life.
3. **System Failures and Safety Standards:** The design and implementation of high-power charging systems must adhere to strict safety standards [3]. System failures could lead to fires or other safety issues, necessitating measures to ensure the system can operate safely in various conditions, including emergency shutdown and fault-handling mechanisms.
4. **Energy Source and Environmental Safety:** If the charging system primarily relies on non-renewable energy sources, it could have adverse environmental impacts.

Ensuring the use of clean, renewable energy sources is a crucial safety issue to reduce the risks of environmental pollution and climate change [4].

References

- [1] J. Robinson, J. Smyth, R. Woodman, and V. Donzella, "Ethical considerations and moral implications of autonomous vehicles and unavoidable collisions," *Theoretical issues in ergonomics science*, vol. 23, no. 4, pp. 435–452, 2022.
- [2] D. Gotterbarn, B. Brinkman, C. Flick, *et al.*, "Acm code of ethics and professional conduct," 2018.
- [3] M. Ragheb, "Risk and safety ethics,"
- [4] T. Muneer, M. Kolhe, and A. Doyle, "Electric vehicles: Prospects and challenges," 2017.

A Appendix A: Points Summary

Task	Requirements	Points
Wireless Charging	Power>50W	6
	Power>100W	4
	Relay protection	3
	Maximum power charging point alignment	2
Free Motion Drive	Motion	10
	Turn around in place	10
Sensor	Obstacle avoidance	5
	Visual recognition of zebra crossing and traffic lights	5
Mechanical Structure	Chassis structure	5
Total	\	50